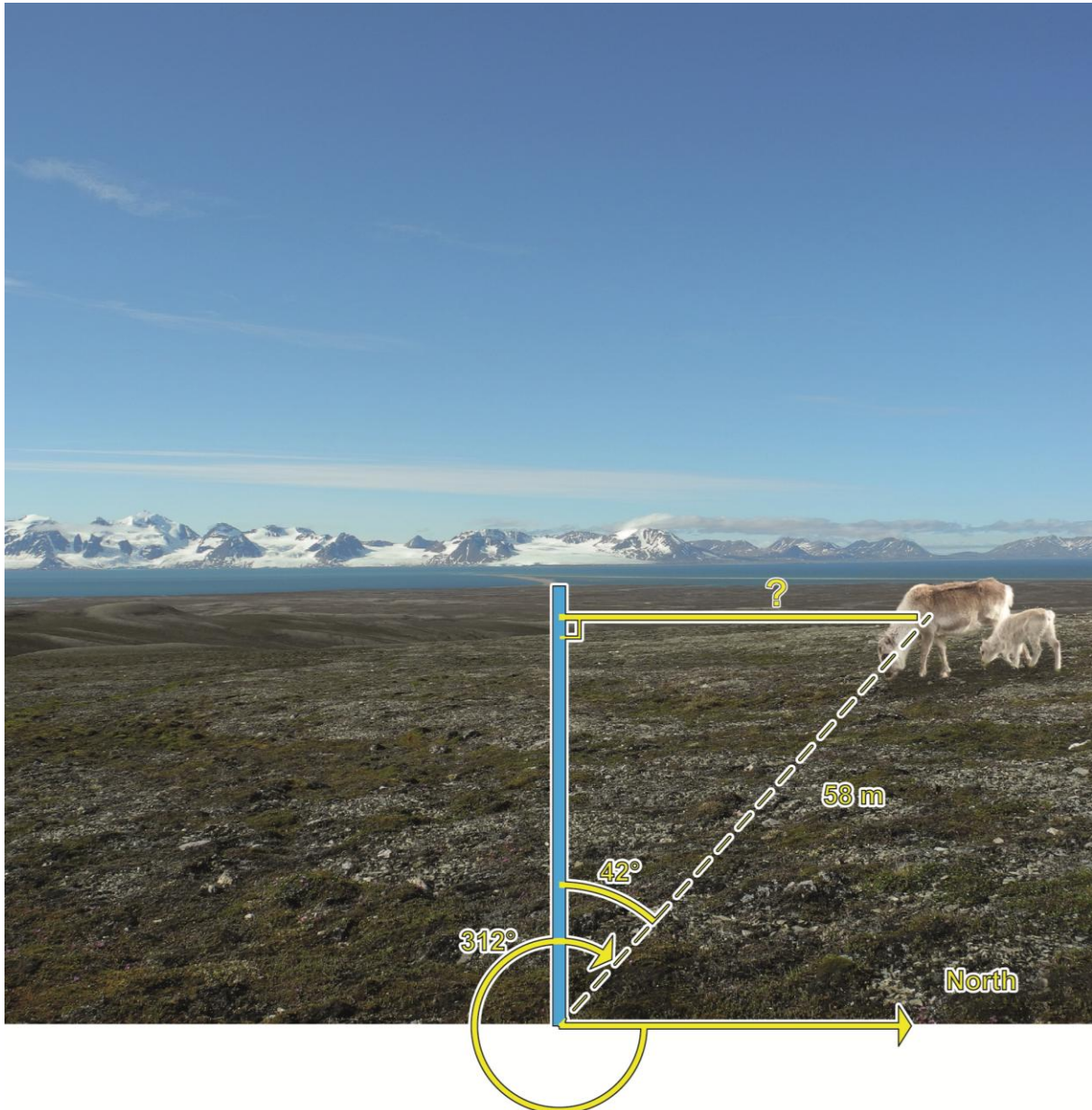


Ungulate population monitoring in a tundra landscape: evaluating total counts and distance sampling accuracy

—
Mathilde Le Moullec

Master thesis in Biology, BIO-3950 - May 2014



Front page and acknowledgement pictures: Mathilde Le Moullec

Ungulate population monitoring in a tundra landscape: evaluating total counts and distance sampling accuracy

Mathilde Le Moulec

BIO-3950

Master's thesis in Biology

Northern Population and Ecosystems

May 2014

Supervisors

Nigel Gilles Yoccoz, The Arctic University of Norway (UiT)

Åshild Ønvik Pedersen, Norwegian Polar Institute (NPI)

Brage Bremset Hansen, Norwegian University of Science and Technology (NTNU)



Abstract

Researchers and managers are constantly working towards decreasing monitoring uncertainties in order to improve inferences in population ecology. The solitary and sedentary Svalbard reindeer (*Rangifer tarandus platyrhynchus*) inhabit a high-Arctic tundra landscape highly suitable to compare accuracy (precision and bias) of population monitoring methods in the wild. The flexible Bayesian state-space model enabled me to assess uncertainties in estimates of the abundance of four reindeer sub-population time-series. In this environment, Total population Counts (TC) were more precise than Distance Sampling (DS), especially when conducted multiple times during a field season (e.g. Sarsøyra, summer 2013: DS Coefficient of Variation (CV)= 0.11, only one TC CV= 0.06; four repeated TC CV= 0.03). In addition, TC's bias was assumed low once integrated in the state-space model and related to re-sightings of marked animals. Conducting DS alone, without TC as background information, would have estimated wrong reindeer population size because the detection function was sensitive to sample size. However, the similarity in landscape and methodology across the two neighboring DS study sites enabled their observations (n= 143) to be pooled, resulting in more plausible estimates, yet slightly higher than those found through TC. DS is used worldwide and this study illustrates fundamental issues around the minimum sample sizes recommended in literature (n>80) and that the number or length of transects must be sufficient to represent habitat structure (in this particular case the proportion of vegetation). Furthermore, combining multiple sources of available data in a common modeling framework, even with wide standard deviation such as DS, resulted in more precise estimates.

Keywords: Line transects, detection probability, Poisson-Poisson sampling, population size, state-space model, Rangifer.

Résumé

Aussi bien les scientifiques que les gestionnaires cherchent à améliorer les incertitudes inhérentes aux recensements des populations pour ainsi améliorer les inférences en écologie des populations. Le renne du Svalbard (*Rangifer tarandus platyrhynchus*) occupe un habitat aux affinités particulières (i.e. grandes plaines, végétation rase) pour pouvoir comparer l'acuité (précision et biais) des méthodes de recensements des populations sauvages. Le « state-space » modèle Bayésien est flexible et a permis de mesurer les incertitudes de comptages de quatre sub-populations de rennes. Il a également permis de montrer que, dans cet environnement, la méthode de recensement total de la population (TC) est plus précise que celle du Distance Sampling (DS) (e.g. Sarsøyra, été 2013: DS CV= 0.11, un seul TC CV= 0.06; quatre TC répétitions $CV_{2013} = 0.03$). En plus d'être précis, les TC sont supposés être faiblement biaisés d'après cette étude. Ils m'ont permis de mettre en avant le fait que sélectionner le meilleur model du DS en suivant les étapes de sélection, aurait, sans regard critique, donné des estimations erronées. La probabilité de détection du DS s'est montré particulièrement sensible à la taille de l'échantillon. La similarité des paysages et de la méthodologie utilisée dans ces deux sites voisins ont permis de regrouper les observations rendant les estimations plus vraisemblables, même si toutefois, elles restent supérieures aux TC. Le DS est intensément utilisé à l'échelle mondiale et cette étude illustre l'importance fondamentale d'avoir un échantillon de taille minimale ($n > 80$) ainsi que de s'assurer d'avoir suffisamment de transectes pour représenter la structure de l'ensemble de l'habitat étudié (dans ce cas particulier : la proportion de végétation). Rassembler des données de multiples sources dans un model commun, même ayant de large intervalles de confiance comme le DS, résulte en des estimations plus précises.

Acknowledgements

I profoundly thank my three supervisors: Åshild, Brage and Nigel (Gilles), for their never-ending willingness to share their knowledge, and to do so in the most wonderful ways and places. Numerous brainstorming sessions in front of Prince Karls Forland or already in the Jardin de Talèfre were a great way to progress my thinking and make science stick to my skin. I am also grateful for the analysis advice from Dr Vidar Grøtan (NTNU).

I thank the Norwegian Polar Institute (NPI) for the providing of such a great working environment. Thanks also to the Biodiversity, Mapping and Graphic Department, and the Logistic teams in Ny-Ålesund and Longyearbyen. The Svalbard Science Forum (SSF), the Arctic University of Norway (UiT) and NPI made this Master thesis possible by financing and procuring logistics for my long field seasons.

I got the best support from my friends and my family. A particular thank you goes to my dear friend Morgan Bender, but also Lorna little and other friends for the proof reading help. Aino Luukkonen, Marit Rønnig and Bart Peeters, we made an amazing a field team!



Table of Contents

Introduction	3
Methods	7
Study area and reindeer population	7
Data collection	8
Total Counts and repeated Total Counts	9
Distance sampling line transects	9
Data analysis	12
Distance sampling analysis	12
Bayesian state-space model	16
Results	19
Distance sampling	19
State-space model time-series uncertainty	21
Discussion	25
Extreme fluctuations are real fluctuations	25
The more information, the more precise the abundance estimate	26
Total Counts accuracy	27
Distance Sampling sources of errors: detection function	28
Distance Sampling source of error: habitat structure	30
Future implications	31
Conclusion	33
References	35
Appendix I	41
Appendix II	42
Appendix III	43
Appendix IV	44
Appendix V	47
Supplements	49

Introduction

A core question in wildlife population ecology is: How many individuals are in the system, and how many will there be? While there are challenges associated with accurately estimating population size and demographic rates, these parameters are essential to identify causes of population fluctuations (Gaillard et al. 2001, Abadi et al. 2010, Zipkin et al. 2014). Investigation of these underlying causes provide important knowledge of population dynamics (e.g. density-dependence; Sæther et al. 2007; Ahrestani et al. 2013), ecosystem dynamics (e.g. inter-specific interactions ; Marshall et al. 2014), environmental factors (Lindén and Knape 2009) and human influences (e.g. population viability; Brook et al. 2000). Robust parameter estimations allow for a well-developed understanding of the system dynamics in order to meet scientific objectives, sustainable wildlife management and conservation decisions (Yoccoz et al. 2001, Cressie et al. 2009, Singh and Milner-Gulland 2011).

It is essential to take estimated uncertainties into consideration as sources of errors influence the measurement of population size and vital rates. These uncertainties, which can exist at a number of levels (Lebreton and Gimenez 2012), are related to the process variation (demographic and environmental stochasticity) and observational errors (Clark and Bjørnstad 2004, Buckland et al. 2007). Because observational errors are not part of the process variation but inherent to the methodology used, it is important to identify their different sources (Ahrestani et al. 2013). Observational errors can arise from the chosen sampling and analytical method (i.e. assumptions of the design and model used; Seddon et al. 2003; Poole et al. 2013), the observer (Muhlfeld et al. 2006), the sampling time and spatial scale (i.e. detection probability may vary with animal's biological cycle and animal habitat use; Pedersen et al. 2012). Although most studies have unacknowledged sources of errors which affect the resulting population size uncertainties (i.e. credible interval, standard error), recent

works have addressed this issue (Clark and Bjørnstad 2004, Newman et al. 2006, Dennis et al. 2010, Knape et al. 2013, Ahrestani et al. 2013). For example, Lebreton and Gimenez (2012) pinpointed that for methods studying density dependence, “neglecting uncertainties in population size should definitely be abandoned”. Once uncertainties are estimated, the “true demographic fluctuation” (the state variable) could be considered free from potential confounding effects that camouflage predicted variations of population dynamics (Clark and Bjørnstad 2004). Hence, population changes are likely to be detected earlier, which is especially important in the context of a warming climate, habitat fragmentation and changes in landscape use.

Comparing accuracy (reflecting both precision and bias; Williams et al. 2002) of population monitoring methods in the wild (*in situ*) requires highly suitable environments where assumptions of the chosen methods are met. Systematic bias can only be quantified when the real size of the population is known, but *in situ* this is usually not possible (Sutherland 2006). High-Arctic Svalbard (74-81°N, 10-35°E) is home to the wild Svalbard reindeer (*Rangifer tarandus platyrhynchus*). The fragmented and tundra landscape provides distinctive traits and characteristics for analyzing precision and sources of errors in reindeer population monitoring methods. Numerous natural barriers to reindeer movement exist, such as tide water glaciers, ice caps, steep ridges and more recently, year round open water fjords causing fairly stationary and non-nomadic behavior (Aanes et al. 2000). Occasional dispersal or migration occurs, but mainly during winter (Hansen et al. 2010b). Wide open areas (Aanes 2000) and the northern Arctic tundra (Elvebakk 1997) with short, prostrated vegetation characterize the lowlands that reindeer inhabit in summer (Hansen et al. 2010b). Consequently, high visibility enables good detection of reindeer. Furthermore, in Svalbard, reindeer can be closely approached by humans (typically closer than 100 m in summer).

There are long time-series of Svalbard reindeer populations that have used Total population Counts (TC). Four sub-populations on Brøggerhalvøya, Sarsøyra, Kaffiøyra (West coast of Spitsbergen) and in Adventdalen (Central Spitsbergen) are monitored annually (Figure 1). In previous studies, TC have been considered to be precise and unbiased population size estimates (Aanes et al. 2000, Tyler et al. 2008, Hansen et al. 2013), yet this assumption has never been investigated. Worldwide, however, the most common method to estimate population abundance of wild animals is Distance Sampling (Buckland et al. 2004). Distance Sampling (DS) is a method where surveys are conducted along transects (lines or points) and is based on the fact that the probability to detect an animal diminishes with increasing distance from the observer (Buckland et al. 2001). Bias and precision can broadly vary according to how assumptions of a DS survey are met, as well of course as sample size. However, achieving high accuracy using line transects in monitoring of large herbivores is difficult (Marques and Buckland 2003, Morellet et al. 2011). Morellet et al., (2007) asserted that DS systematic bias (not precision as they termed it) is largely unknown, due to few studies assessing performance of DS line transect methods using populations of known size (however see Porteus et al. 2011 for such an example).

The Bayesian statistical framework has made it possible to integrate data collected using different methods and thus combine data with different uncertainties. The information extracted from the available data enabled higher precision of parameter estimates and missing census can even be estimated (Clark and Bjørnstad 2004, Abadi et al. 2010). Knape et al (2013) and Dennis et al., 2010 proposed that one key method to evaluating precision of population counts was to perform repeated counts. Further, even if counts repeated within a field season are only occasionally conducted along the time series, parameter estimates and likelihood functions are significantly improved (Dennis et al. 2010).

In this study, I *i*) estimated Svalbard reindeer abundance using DS line transect data from two study locations in summer 2013 and *ii*) integrated this information with TC and repeated TC (summer 2009 and 2013) to estimate abundance uncertainties. To achieve this, I used a Bayesian state-space model for four different reindeer sub-populations. Finally, I *iii*) compared and discussed sources of errors and precision of TC versus DS.



Figure 1. Map of the Svalbard archipelago (74-81N, 10-35E) and the four study sites.

Methods

Study area and reindeer population

Svalbard reindeer data was collected from the Northwest and central part of Spitsbergen, Svalbard in four study sites (Figure 1). Brøggerhalvøya, Sarsøyra and Kaffiøyra are peninsulas separated by tide water glaciers, and are inhabited by three distinct sub-populations of reindeer. Adventdalen, close to the settlement of Longyearbyen (78°13'N, 15°33'E), is a wide inland valley connected with several side valleys (~175 km² below 250m) (Tyler et al. 2008). The other sites were confined below 200m in altitude, which is dominant reindeer habitat during summer and moraines and glaciers were excluded. The two northernmost study sites, Brøggerhalvøya (~88km²) and Sarsøyra (40 km²), close to the Ny-Ålesund scientific base (78°55'N, 11°55'E), were described by Hansen et al. (2009). Kaffiøyra (35 km²) is situated southward of Sarsøyra and both sites are characterized by large plains of tundra where the two dominant vegetation types are “pioneer vegetation” (41%, class 8) and “established *Dryas* tundra” (39%, class 14). Vegetation maps were derived from remote sensing data (Johansen et al. 2012) (Figure 2).

Svalbard reindeer were re-introduced in the area of Ny-Ålesund in 1978. Twelve reindeer were imported from the Adventdalen valley and released on Brøggerhalvøya (Aanes et al. 2003). The Svalbard reindeer is the only large herbivore present on the archipelago and population size has been identified to be strongly controlled by the availability of food resources (Aanes et al. 2000). During the harsh winter of 1993/1994, the population crashed because of heavy icing, “rain-on-snow” events (ROS; Rennert et al. 2009, Constable et al. 2014) that caused locked pastures and depletion of food resources due to high densities of reindeer in a small area. The reindeer population suffered high mortality and emigrated southwards to Sarsøyra (1994), and afterwards, to Kaffiøyra (1996). Svalbard reindeer do not

experience significant predation (Derocher et al. 2000) and are not hunted in the four sub-populations.

Data collection

Existing time-series of summer TC of Svalbard reindeer, from the four study locations (Figure 1), were used in combination with repeated TC conducted during the course of a single field season (Table 1). Although winter TC did exist from the time of the reindeer re-introduction on Brøggerhalvøya (Aanes et al. 2000, 2002, 2003, Kohler and Aanes 2004, Hansen et al. 2011), I decided to use summer time-series that existed in all study sites with some years having repeats. Moreover, uncertainties could be compared across sites as winter and summer TC have different sources of error, i.e. reindeer use habitats higher in altitude in winter (Hansen et al. 2009a, 2010a). Finally, reindeer from Sarsøyra and Kaffiøyra were also sampled by line transects in summer 2013.

In addition to TC and DS data, I used information on numbers of VHF collared females (1999-2000) and marked females (2000) sighted during censuses (see Hansen et al. 2009a; Hansen et al. 2010a for details) to support assumptions.

Table 1. Summary of the Svalbard reindeer data available for the four study areas during summer. Number of repeats are indicated in parentheses.

Study area	Total Counts	Repeated Total Counts	Distance Sampling
Brøggerhalvøya	1979-present	2009 (2) 2013(2)	-
Sarsøyra	2000-present	2009 (4) 2013(4)	2013
Kaffiøyra	2002-present	2009 (2)	2013
Adventdalen	1979-present	2001-2007 (2)	-

Total Counts and repeated Total Counts

Total population Counts and repeated TC were performed in the middle of the summer (July-August). The stationary behavior of reindeer, which experience very low rates of mortality during summer (Reimers 1983), met the assumption of constant abundance inside an area during the same field season (no inter-population exchange), so that repeated total counts estimated the same population size. Two consecutive counts were separated by a minimum of four days to ensure re-distribution of reindeer in the landscape. Sarsøyra and Kaffiøyra reindeer were counted by two to four observers, and always by four in the repeated TC, in a single day. Brøggerhalvøya required two observers for two consecutive days which were separated by a natural barrier i.e. polar desert. Approximately parallel walking routes, covering the entire sites were similar between the years and routes were switched between observers when performing repeated counts. Individual or groups positions (clusters) of reindeer were located on a map. Observers communicated with each other through VHF radio to reduce the potential for double counts. The Adventdalen valley demanded four to six observers during a week of field work and part of this time-series has been used in Hansen et al. (2013). Repeated TC from 2001-2007 were extracted from Tyler et al. (2008) and independently and similarly conducted to TC from this study.

Distance sampling line transects

Distance Sampling data were collected in Sarsøyra and Kaffiøyra along transects representing a total line length of 19029m and 14937m respectively. The first principle of DS methodology is that detection probability of reindeers on the line (distance = 0) must be certain (assumption 1). Second, the distance of each observation to the line should be recorded at the original position of the animal when detected (assumption 2) and third this should be done with

accuracy (assumption 3), avoiding systematic measurement bias (Buckland et al. 2001). Thus, it was important that data were not pooled into distance intervals in the field.

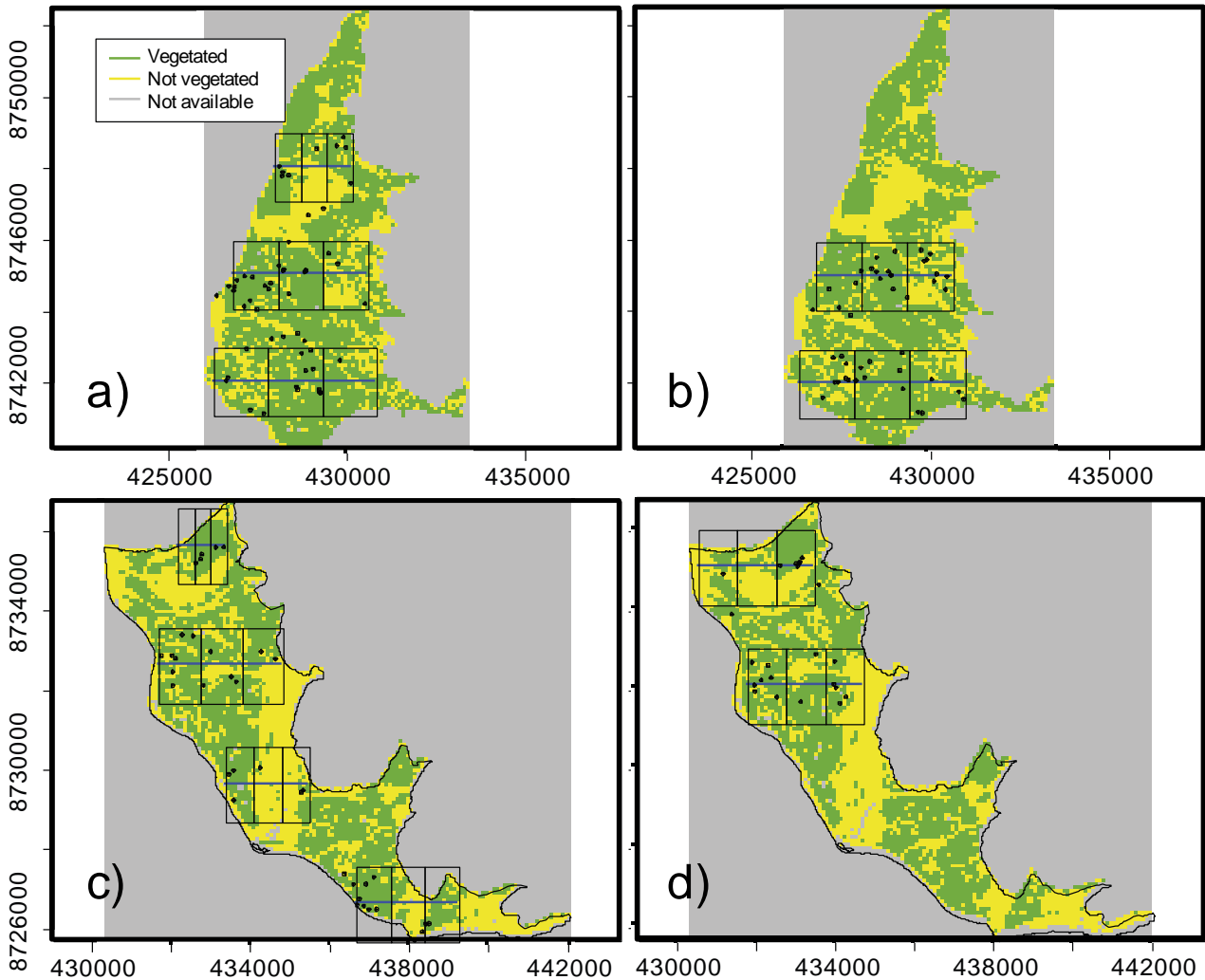


Figure 2. (a and b) Vegetation maps of Sarsøyra (40 km²) and (c and d) Kaffiøyra (35 km²), with blue horizontal lines representing the distance sampling transects. Each line is divided into 3 segments (one segment is interpreted as one transect); black rectangles on each side of the line represent the width of the covered area (953 m i.e. 5% of the data truncation). The black points represent cluster positions. Each map represents one sampling day. See *Methods* for details on vegetation classes.

Study design

The first way to avoid introducing observation error was to randomly sample the study site. However, care should be taken if a density gradient in the animal's distribution exists in the landscape. Then the survey should be designed to avoid any gradient parallel to the lines, otherwise, precision might be lower (Marques et al. 2012, Barabesi and Fattorini 2013). Transects were drawn perpendicular to the potential gradient that could exist, following altitudinal flowering plant phenology (Hansen et al. 2009b). Thus, transects were crossing from the mountains to the sea, corresponding to an East/West orientation. One latitude was randomly chosen and other lines were placed 3km apart North and South from this latitude for each DS survey. This was a sufficient distance to avoid overlap and accordingly, avoid violation of independence (Royle et al. 2004). For the same independence requirement, one observation does not correspond to a single reindeer but the cluster it belonged to (Buckland et al. 2001, Guillera-arroita et al. 2012). One study site was covered in one day.

Measurements in the field

I performed DS walking at constant speed along each line transect and no stops were made to scan surroundings. When a reindeer or cluster was spotted, glances only in its direction were made until measurements were finished. The position of the observer was marked for possible distance to the line correction. In a cluster, distance was measured on the reindeer that was furthest to the left (as observed by the naked eye) with laser binoculars Leica Geovide (42x10). In case of calf presence, the distance was measured on the mother. If the reindeer cluster were standing further than the maximum distance the laser can measure (~700m) positions were marked on a map. Binoculars were not used to search for reindeer and if a new reindeer was sighted while using them, or the group was bigger than first counted, those reindeer were excluded from further analysis. Finally, the angle toward the animal was measured with the stable SILVA JET 5 compass.

Data analysis

Distance sampling analysis

Since each distance sampling repeat had unique randomly drawn walking routes, data from the same study sites were pooled and information at the sample unit (a line) conserved (e.g. covariates characteristic of the line). Partitioning each of the transects in 3 equal segments decreased habitat heterogeneity and augmented study units (e.g. one partitioned line) according to Royle et al. (2004). A total of 33 transects (Sarsøyra: 15 lines 728-1544m, Kaffiøyra: 18 lines 107-1047m) were used in the analysis (Figure 2). The conventional distance sampling likelihood from Buckland et al (2001) was adapted to include habitat covariates likely affecting abundance (Royle et al. 2004) and detection (Sillett et al. 2012). The proportion of vegetated area (pixel types from class 8 to 18; Johansen et al. 2012) over the total covered area (all pixel types from 1 to 18) was extracted from a digital vegetation maps (Figure 2). The vegetation proportion predictor was also transformed to the logarithmic scale as well as a quadratic polynomial (Sillett et al. 2012). The sampling site (Sarsøyra or Kaffiøyra) was also included as a factor. Analyses were conducted in R 2.15.3 with the unmarked 0.10-2 package (Fiske and Chandler 2011). The *distsamp* function was used with the multinomial-Poisson mixture (Royle et al. 2004, Fiske and Chandler 2011) to model density and detection probability and results predictions used the function *predict* (Fiske and Chandler 2011). GIS computations were completed in R.

Statistical methods

First the data was checked for possible spatial clumping of animals using the variance estimation of the sample size (Buckland et al., 2001) (Appendix I). Spatial distribution of reindeer abundance was modeled as a Poisson random variable with expected number of animals N_i in the total study area equal to $E[N_i] = \lambda_i$ and described as: $N_i \sim P(\lambda_i)$. Hence, a detected cluster could occur at any position in the covered area.

Theoretical explanations to get to the statistical formulation of density estimates \widehat{D}_i are described in detail in appendix II. Here, (L_i) was the length of the transect i and $f(0)$ was the probability density function of the perpendicular distance data at distance 0 m where all animals are supposed to be detected (Buckland et al. 2001).

$$\widehat{D}_i = \frac{\lambda_i \cdot f(0)}{2L_i} \text{ clusters/km}^2$$

The detection function depended on each observation perpendicular distance x_i to the line i . The half-normal, hazard-rate and uniform key functions were tested as different forms of the detection function. The half-normal key $g(x_i | \sigma_i)$ is defined by:

$$g(x_i | \sigma_i) = \exp\left(\frac{-x_i^2}{2\sigma_i^2}\right) \text{ where } \sigma_i \text{ is the half normal parameter shape of transect } i \text{ (Figure 3).}$$

The available covariates Z_i of transect i were related to the detection parameter σ_i and mean density parameter λ_i on a logarithmic scale (Royle et al. 2004, Fiske and Chandler 2011):

$$\log(\sigma_i) = \alpha_0 + \alpha_1 Z_i$$

$$\log(\lambda_i) = \beta_0 + \beta_1 Z_i$$

Distances were measured on a continuous scale. Pooling data into bins of j distance intervals permitted the detection function to integrate cell probabilities π_{ij} of a transect i over each intervals j as multinomial trials (Sillett et al. 2012). y_{ij} was the number of individuals detected at transect i and interval j : $y_{ij} \sim \text{Multinomial}(N_i, \pi_{ij})$.

Objects occurred in clusters, thus, density extrapolation to the total study surface (A) took into consideration the expected average cluster size \bar{S} (common for both sites). Abundance was estimated as: $\widehat{N}_{DS} = A \cdot \widehat{D} \cdot \bar{S}$. Finally, abundance estimation was repeated using 500 bootstrapped replicates to calculate the mean abundance μ_{DS} and the standard deviation sd .

Model selection

Different model combinations with abundance and detection covariates analyzed in a half normal, hazard rate or uniform detection function, resulted in 63 candidate models (Appendix III). From this first list, 37 models did not include the sampling site effect on the detection function (Appendix III). The two “model list” followed the three model selection procedures as described below:

- (1) I explored several distance interval combinations (equal interval 60m or 130m or unequal interval) (Buckland et al. 2001). Model lists were run for each distance interval combination and the three best models based on Akaike’s Information Criterion (AIC) of each combination were retained.
- (2) To find the distance interval combination having the best goodness of fit for the model, I applied a Freeman-Tukey test for the models selected in (1). This test does not require pooling intervals with small expected values together (Brooks et al. 2000, Sillett et al. 2012). The Freeman-Tukey statistic h^2 measured difference in fit between the observed data y_{ij} and the expected value e_{ij} at transect i and interval j as follows:

$$h^2 = \sum_{ij} (\sqrt{y_{ij}} - \sqrt{e_{ij}})^2$$

500 Bootstrap samples were used and the distance interval combination with the highest fit (corresponding to the lowest value of h^2) was chosen.

- (3) Once the distance interval combination was selected, the last step retained the best model ranked by AIC value. The AIC_C , another model selection criterion widely used in ecology, was also calculated for comparison. AIC_C provides greater penalty for additional parameters and account for the sample size. Although Burnham and Anderson (2002) recommend to use AIC_C , the statistical literature is not that clear on this topic (Claeskens and Hjort 2008) and AIC was preferred for selecting the model.

Table 2. Ranking of the three best detection models for estimating Svalbard reindeer density, according to the AIC and relative AIC difference (ΔAIC), for model list 1 (vegetation proportion and study site were density and detection covariates, 63 models, see appendix III) and model list 2 (the study site was not a detection covariate proposed, 37 models from model list 1, see appendix III). Model selection procedure investigated three distance interval combinations: Equal intervals every 60 m, equal intervals every 130 m and unequal intervals (composed by 10 cut points: $5 \times 60 \text{ m} + 4 \times 100 \text{ m} + (\text{Distance}_{\text{Max}} + 100 \text{ m})$). Freeman-Tukey test was bootstrapped with 500 iterations. The bootstrap outcome mean statistic value = h^2 , standards deviation = $sd(h^2)$ and P-values are presented. Hn = Half normal key functions, Hz = Hazard rate, numbers of models' parameters = Par. Bolted numbers are related to steppe (2) and (3) from the DS model selection section (see text).

Intervals	Model list	Model	Par	h^2	$sd(h^2)$	P-value	AIC	ΔAIC
Equal 60	List 1	Hn_21	5	128.39	7.34	0.40	633.74	0.00
		Hn_20	6	127.64	7.24	0.37	634.02	0.28
		Hz_38	4	128.15	7.87	0.38	634.07	0.33
	List 2	Hz_38	4	128.15	7.87	0.38	634.07	0.33
		Hz_39	4	128.37	7.87	0.39	634.35	0.61
		Hz_41	5	128.13	7.24	0.38	635.96	2.22
Equal 130	List 1	Hn_21	5	82.02	5.92	0.19	461.43	0.00
		Hn_20	6	81.85	5.75	0.17	461.71	0.28
		Hn_26	7	80.79	5.90	0.18	462.46	1.03
	List 2	Hn_8	3	84.39	6.12	0.25	463.34	1.91
		Hn_9	3	83.87	5.32	0.16	463.63	2.20
		Hz_38	4	84.29	5.87	0.26	463.89	2.46
Unequal A	List 1	Hn_26	7	103.10	5.83	0.45	534.94	0.00
		Hn_21	5	104.46	6.21	0.43	534.95	0.01
		Hn_20	6	103.53	6.19	0.38	535.23	0.29
	List 2	Hz_38	4	104.54	5.89	0.34	535.74	0.80
		Hz_39	4	104.68	5.81	0.37	536.03	1.09
		Hz_41	5	104.37	5.69	0.33	537.63	2.69

Bayesian state-space model

Reindeer population TC time-series were fitted using a state-space model that simultaneously integrated repeated Total Counts (within one season) and Distance Sampling analysis. The state-space modeling was performed in a Bayesian framework (Kery and Schaub 2012). Likelihood from the census time-series can be decomposed in two distinct components of the system: a process and an observation equation. This hierarchical view of the state-space model structures the “model building” (Royle and Dorazio 2008). Such a model can deal with hidden state variables or missing values (Clark and Bjørnstad 2004).

The process equation was of Markovian type and linked reindeer population size fluctuation through the years: the true abundance N_{t+1} depended on the previous abundance N_t (corresponding to n_t on the logarithmic scale)(Kery and Schaub 2012). The growth rate λ_t , on the logarithmic scale r_t , were normally distributed with mean \bar{r} and the process variance σ_r^2 corresponding to environmental and demographic stochasticity:

$$\begin{aligned} \log(N_{t+1}) &= \log(N_t) + \log(\lambda_t) \\ \Leftrightarrow n_{t+1} &= n_t + r_t \quad \text{and} \quad r_t = \mathcal{N}(\bar{r}, \sigma_r^2) \end{aligned}$$

The observed equation linked observed data Y_t to the true state of the process N_t (true population size). The sampling distribution was a Poisson sampling (Dennis et al. 2010) instead of a binomial sampling which is commonly used (Royle and Dorazio 2008):

$$Y_t = P(N_t)$$

Although binomial sampling does not allow for false positive counts (Kery and Schaub 2012), the Poisson sampling does (Muhlfeld et al. 2006). Double counts (false positive) were potential sources of error in the system and neglecting to account for these could have underestimated population size estimates. However, because the false positive rate remained unknown, the Poisson distribution does not allow quantification of the observation process (i.e. systematic bias and observation errors) (Clark and Bjørnstad 2004, Newman et al. 2006).

Repeated TC were independently analyzed in the same way where k indicates the number of repeats (Dennis et al. 2010):

$$Y_{t,k} = P(N_t).$$

A Normal distribution was used to integrate Distance Sampling data to the state-space model in year 2013:

$$\mu_{DS} = \mathcal{N}(N_{2013}, sd)$$

Although, one should note that Winbugs used $\frac{1}{sd^2}$ to define the standard deviation of a normal distribution. The estimator μ_{DS} and its standard deviation sd resulted from the bootstrap procedure in Unmarked (see above).

Priors are usually kept uninformative (Kery and Schaub 2012), however, as the first year was not defined in the process equation, the prior for the initial population size corresponded to the logarithm of the first abundance census with a variance of 0.01. Other priors were kept vague. Thus, the prior assumed a non growing population with a mean growth rate \bar{r} defined as: $\bar{r} = \mathcal{N}(0, 0.001)$, and the prior for the process variance σ_r^2 was described as: $\sigma_r^2 = \text{Unif}(0, 1)$.

Finally, the posterior distribution was obtained using Markovian Chain Monte Carlo (MCMC) techniques computed from R2.15.3 to Winbugs1.4.3 software with three MCMC chains, 100 000 iterations and 2000 burn-in (first part of the chains discarded). Estimates obtained represented a sample from the posterior distribution. In addition, the 2.55th to 97.55th percentiles of the posterior distribution corresponded to the 95% Credible Interval (CI) (Bayesian confidence interval; Kery and Schaub 2012). Nonetheless, to easily compare precision with different data input (one to four TC and/or DS or no data included in 2013, Table 4), the posterior standard deviation and Coefficient of Variation (CV) were preferred. The posterior distributions were plotted (Figure 4) and level of convergence of the chains (Rhat) available in Appendix IV.

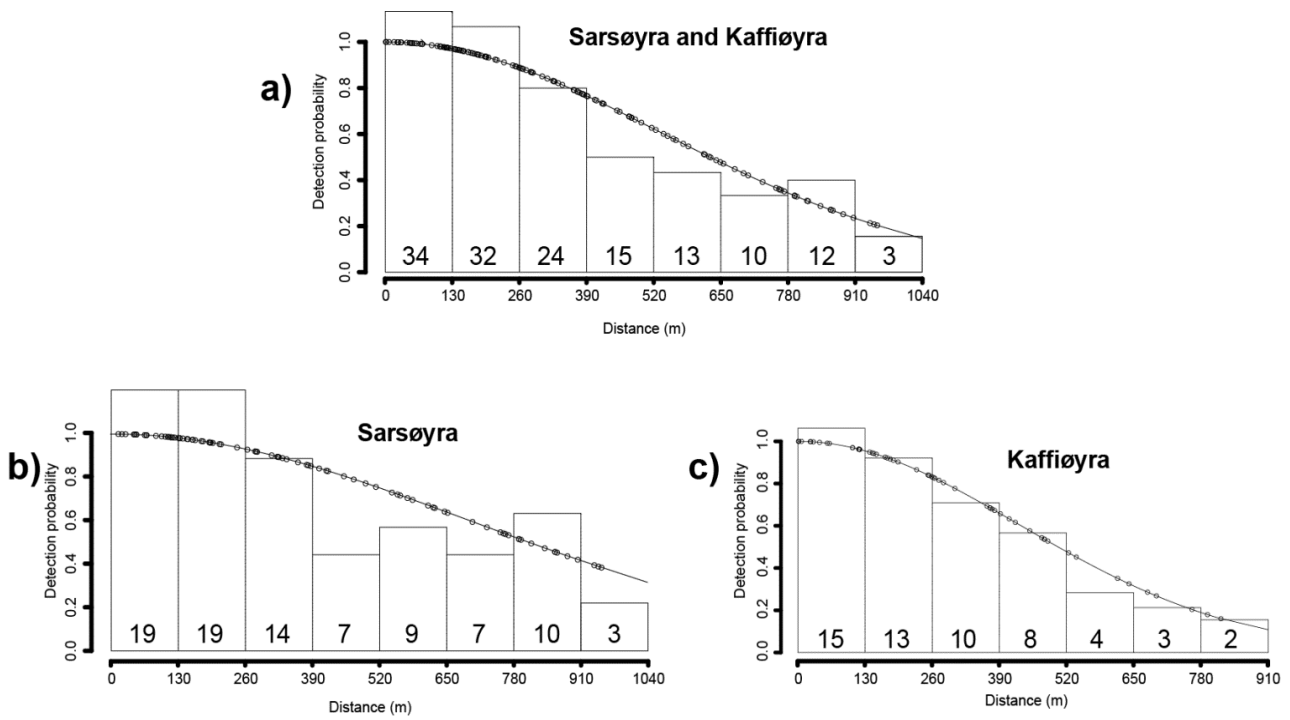


Figure 3. Distance sampling histograms of the number of clusters observed per distance interval (numbers are given at the bottom of the bars) and the half normal detection function probability from (a) model Hn_8 and (b and c) model Hn_21. Model Hn_8 pooled Sarsøyra and Kaffiøyra sites for the detection function estimation while Hn_21 separated them (see text for further details). Each observation distance to the line is plotted on the top of the detection curve.

Results

Distance sampling

Following exploratory data analysis guidelines provided by Buckland et al. (2001), I right-truncated 5% of the furthest observations from the line (Sarsøyra and Kaffiøyra data pooled) resulting in a low variance (Appendix I). Higher truncation percentage did not decrease the variance. Accordingly, the furthest observation from the line was at 953m. This distance defined the width of the 33 covered area (area surveyed along the lines) where surface vegetation was calculated (ranging from 0.43 to 2.89 km²). The vegetation maps (see *Methods*, Johansen et al. 2012), indicated that the proportion of vegetation inside the covered area (69.6% and 54.1% for Sarsøyra and Kaffiøyra respectively) was slightly higher (from about 3.5% times more) than the vegetation proportion of the total study area (66.1% and 50.5% for Sarsøyra and Kaffiøyra). When study sites were pooled, clustered observations amounted to 143 animal groups (n=88 and n=55 in Sarsøyra and Kaffiøyra respectively). More than 30 observations in the first distance intervals were close to the line but less than 20 were, when sites were distinguished (Figure 3).

The Freeman-Tukey goodness of fit statistics (h^2) were lowest for the 130m distance interval, thus, this was evaluated as being the best cut point combination (<80.8 in model list 1 and <84.4 in model list 2 for the 3 best models based on AIC; Table 2). Moreover the h^2 test indicated no significant lack of fit ($p>0.16$ in all models) (Royle et al. 2004). When pooling observations from both sites, histograms of the frequency of observations per 130m distance interval (Figure 3) had a “well behaved” shape as recommended by Buckland et al. (2001). Indeed, the detection probability diminished, with a shoulder around 400m and smoothly decreased until 953m (following a “shape criterion” curve; Buckland et al. 2001). When detection was separately considered in each site, the patterns were slightly different and detection probability was lower on Kaffiøyra (Figure 3). On Sarsøyra, observations decreased

in two steps at 390m and 910m, with no decrease between those steps. However, on Kaffiøyra, observations decreased earlier (from 130m) and, more regularly until 819m, yet at 520m, detection dropped more than half (from 10 to 4 clusters detected) (Figure 3).

Table 3. Parameter estimates with asymptotic standard error in parentheses from the selected detection models of the distance sampling analysis (Table 2). σ was the detection parameter and λ the mean density parameter on the logarithmic scale. The estimated mean abundance \hat{N} and its standard deviation were bootstrapped 500 times.

Coefficient	Model Hn_21	Model Hn_8
<u>Density ($\ln \lambda$)</u>		
Intercept	0.16 \pm 0.39	-0.06 \pm 0.38
Vegetation	2.09 \pm 0.57	2.02 \pm 0.53
Region (Sarsøyra)	-0.41 \pm 0.23	-
<u>Detection ($\ln \sigma$)</u>		
Intercept	5.94 \pm 0.11	6.19 \pm 0.09
Region (Sarsøyra)	0.42 \pm 0.18	-
<u>Abundance (\hat{N})</u>		
Sarsøyra	199 \pm 33	257 \pm 28
Kaffiøyra	265 \pm 40	174 \pm 19

The most parsimonious model based on AIC was a half normal key function with vegetation proportion and sites as additive covariates influencing density, and sites influencing the detection function (model Hn_21, Table 2, Appendix III). The best model that did not account for the study sites as a detection covariate was also modeled by a half normal key function (model Hn_8, Table 2, appendix III). Only the vegetation proportion on normal scale influenced the density estimation of model Hn_8. The Δ AIC between those two models was 1.92 (Table 2). However, calculating the Δ AICc reduced the difference in parsimony (AICc for model Hn_21= 463.65 and AICc for Hn_8= 464.17, Δ AICc = 0.52). The proportion of vegetated area strongly influenced the predicted density of reindeer of both model Hn_21 and Hn_8 (Table 3). Hence, if 50% of the transect surface is vegetated, for example, model Hn_8 predicts a density of 2.59 ± 0.38 clusters/km². If 90% of the surface is vegetated, the

density increases to 5.80 ± 0.91 (Appendix V). The mean number of reindeer per groups observed with naked eyes after data truncation was $\bar{S} = 1.64$. The total abundance estimates of model Hn_21 was different and less precise than model Hn_8 (see Table 3). The estimated abundance and standard deviation from model Hn_8 were $\mu_{DS} = 256 \pm 27.25$ [R package unmarked abundance \pm sd] and $\mu_{DS} = 174 \pm 18.83$ on Kaffiøyra (Table 3 and Figure 4).

State-space model time-series uncertainty

The observed total counts and estimated \widehat{N}_t values from the Bayesian posterior distribution were rather close (Figure 4), although \widehat{N}_t tended to smooth extreme variations in the observed time-series. For example, in summer 2002 on Brøggerhalvøya 65 [49:83] (posterior mean \widehat{N}_t [95% credible interval]) reindeer were estimated while 52 were counted, but the estimated credible intervals always included the observed TC. One exception of a repeated total count outside the CI existed in 2013, on Sarsøyra (estimate = 223 [209:237], 1st out of 4 repeats = 241 reindeer). Distance Sampling abundance estimates obtained through R package unmarked were not included in the credible interval from the Bayesian state-space model, but the lower part of the standard deviation was (Figure 4). One should recall that although DS density estimates come with a wide standard deviation, one TC alone has no measure of uncertainty.

The credible intervals were reduced during years when repeated samplings were included in the state-space model. This was illustrated by the dashed vertical lines in Figure 4. The models were run with different data available in 2013 (Table 4) so that I could explicitly compare the precision state estimate. Unreliable estimates were obtained when data was missing; especially if consecutive counts were missing such as would be the case on Kaffiøyra, if 2013 was removed. Including DS alone sharply improved the precision of the estimates. Note that one single Total Count in 2013 gave different, but more precise results than one single DS. When repeated total counts were conducted, standard deviation further decreased (2009 Sarsøyra 4 repeated TC: $154 \pm [142:166]$ CV=0.04; 2009 Kaffiøyra 2TC:

156 ± [140:173] CV=0.05; see table 4 for 2013). Because four TC resulted in very precise estimates, adding DS in 2013 on Sarsøyra only improved the precision slightly. Nonetheless, the most precise estimates integrated all data available.

The mean CV over the full Adventdalen time-series was precise (0.04). During the seven consecutive years of independent, replicated TC in Adventdalen, the CV was slightly improved from 0.03 (mean CV without replicates) to 0.02 (with replicates).

All four study sites were subject to strong fluctuations in population size. A major population decrease happened on Brøggerhalvøya, Sarsøyra and Adventdalen during 2001 to 2002 ($r_{\text{Brøgger}} = -0.95 \pm [-1.26:-0.65]$, $r_{\text{Sarsøyra}} = -0.35 \pm [-0.58:-0.13]$ and $r_{\text{Adventdalen}} = -0.33 [-0.40:-0.27]$ [posterior mean r_t : CI]) (appendix IV) when the first count was performed on Kaffiøyra with the lowest abundance estimated for that population (96 [78:115]). In all sites, large positive growth rate followed straight after the 2002 crash (for 2003: $r_{\text{Brøgger}} = 0.62 \pm [0.31:0.92]$, $r_{\text{Sarsøyra}} = 0.31 \pm [0.09:0.54]$, $r_{\text{Kaffiøyra}} = 0.27 \pm [0.04:0.50]$ and $r_{\text{Adventdalen}} = 0.30 [0.23:0.37]$, appendix VI). For example, on Brøggerhalvøya, the population approximately doubled (TC: 52 to 125 reindeer, estimated TC: 64 [49:83] to 119 [100:141] in 2002 and 2003, respectively).

Only three counts with less than 30 reindeer from 1979-1981 on Brøggerhalvøya were followed by seven years without censuses, which prevented MCMC chains to converge with the upper bound of the CI up to 8500 individuals. Therefore, the time-series used in this study started in 1988 with 194 reindeer. MCMC chains still did not converge for the 5 and 3 successive TC missing from 1990-1994 and 1996-1998 (maximum lack of convergence obtained in 1996, $R_{\text{hat}}=0.007$, appendix IV). On Brøggerhalvøya, when summer censuses were conducted, abundance was high from 1988 to 2001 (Figure 4). After 2003, the population size in summer was approximately half the size compared to that before the 2002 crash. Since then, Sarsøyra has shown two peaks in 2005 and 2013. Kaffiøyra had the

strongest oscillating pattern despite data missing in recent years (2011 and 2012); crashes of similar amplitudes appeared in 2006 and 2010 ($r_{2006} = -0.30 \pm 0.11$, $r_{2010} = -0.25 \pm 0.10$), i.e. following winters with extremely poor feeding conditions due to heavy ROS and icing (Hansen et al. 2010, 2011).

Females reindeer with VHF collar were tracked intensively during two field seasons and 97.5% (1 out of 42; 42 correspond to 19 females in summer 1999 plus 23 in summer 2000) stayed in their respective site. One animal crossed the bay between Brøggerhalvøya and Sarsøyra in July 2000. Before the census of August 2000, 27 females (VHF marked) were known as present in the study site. All of them were sighted during the TC. During the same census, one out of 53 (VHF and marked) animals was counted twice (1.9%).

Table 4. Abundance estimates: mean of posterior distribution (\hat{N}), standard deviation (sd) and credible interval (CI) obtained using a Bayesian state-space model fitted with different data combinations from three study sites in 2013. The Coefficient of Variation (CV) correspond to \hat{N} divided by sd. NA= count removed from data; TC = Total Count; 1st TC= the first TC from the 2013 field season; DS= Distance Sampling. Models with the most TC repeats were used for comparison with DS. The full time-series estimates of the bolded row are available in appendix IV.

Study site	Data source	\hat{N} (2013)	sd	CI	CV
Brøggerhalvøya	NA	93	41	[39:193]	0.44
	1 st TC	131	11	[110:154]	0.08
	2 TC	122	8	[107:137]	0.07
Sarsøyra	NA	181	57	[96:314]	0.31
	DS	241	27	[189:294]	0.11
	1 st TC	237	15	[208:268]	0.06
	DS + 1 st TC	242	13	[216:268]	0.05
	4 TC	221	7	[206:235]	0.03
	DS + 4 TC	223	7	[209:237]	0.03
Kaffiøyra	NA	171	364	[32:528]	2.13
	DS	171	19	[134:207]	0.11
	1 TC	144	12	[122:168]	0.08
	DS + 1 TC	153	10	[133:174]	0.07

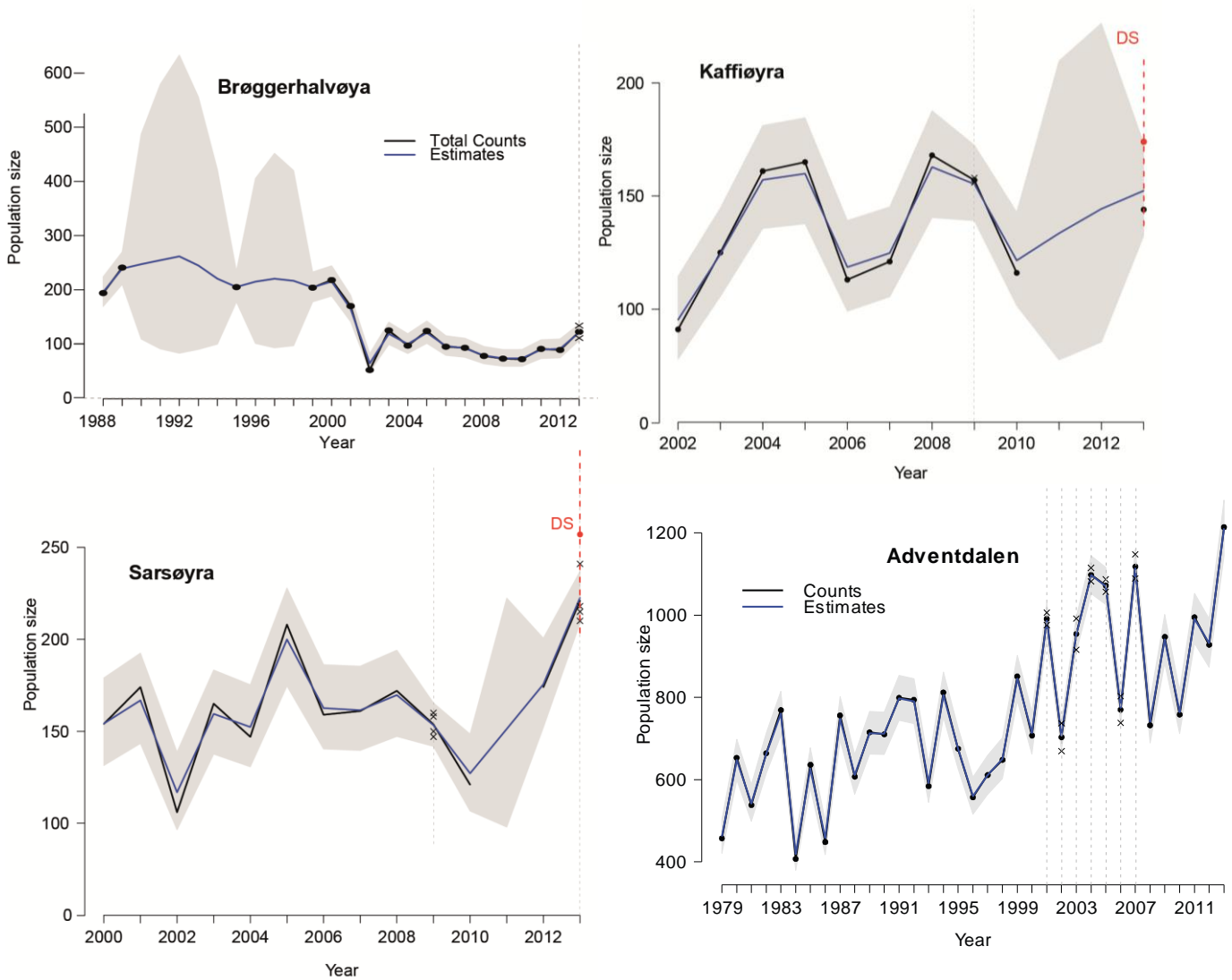


Figure 4. Mean Bayesian posterior distribution of estimated population size (blue line) and its corresponding 95% credible interval (grey polygons) for summer total counts for the four study sites: Brøggerhalvøya (top left), Sarsøyra (bottom left), Kaffiøyra (top right) and Adventdalen (bottom right). The TC of reindeer are represented by a black dot (missing for Sarsøyra) linked by the black line. Repeated TC is symbolized by a cross and indicated by a dashed vertical line. Dashed red segments are the confidence intervals ($\pm 1.96 \times$ standard deviation) associated with the estimated abundance (red dot) from the distance sampling analysis in R package unmade in Table 3.

Discussion

In the present study, I have used time-series of strongly fluctuating sub-populations of high-arctic Svalbard reindeer to investigate abundance uncertainties, and how uncertainties varied between two sampling methods, TC and DS. The Bayesian state-space model made it possible to successfully combine TC, repeated TC (within one field season) and DS in a common framework. The inclusion of more data, even with wide standard deviation such as DS, resulted in more precise estimates (Figure 4). In particular, the Bayesian approach enabled direct comparisons of the precision of both sampling methods and showed that TC was more precise than DS (Table 4). Having TC estimates as a baseline for comparison (i.e. assuming they were close approximation to the “true” population size), emphasized that blindly following DS model selection would have led to erroneous estimates. Finally, reindeer density was found to be highly correlated with vegetated surface (Table 3), thus illustrating the importance that habitat structure of the area covered by DS must be representative of the total study site.

Extreme fluctuations are real fluctuations

Studies based on TC have demonstrated that the population size of Svalbard reindeer fluctuates greatly between years (Solberg et al. 2001, Aanes et al. 2003, Tyler et al. 2008). Reduced population growth is typically associated with winter “rain-on-snow” events (ROS, see *Methods*) and is also more prominent when reindeer occur at high density, that is, a negative first-order density dependence (Aanes et al. 2000, Solberg et al. 2001, Kohler and Aanes 2004, Tyler et al. 2008, Hansen et al. 2011). In contrast, strong positive growth rates are associated with an absence of ROS events and high quality of the grazing grounds the previous summer (i.e. low grazing pressure and large plant biomass production linked with high summer temperature; van der Wal and Hessen 2009; van der Wal and Stien in press).

Svalbard reindeer have a single offspring, so that when these conditions are met, close to all adult female reindeer can have one calf (Øritsland 1985 reported rates up to 95%).

Nevertheless, extreme positive growth rates, such as those observed from 2002 to 2003 in Brøggerhalvøya, when the reindeer population more than doubled, were biologically impossible if the population was isolated. Actually, partial migration occurred between sites, especially during harsh winters (Hansen et al. 2010), influencing growth rates. This study did not constrain growth rate or set a first-order density dependence parameter in the statistical model, because additional uncertainties associated with the extra parameter would then be introduced. These parameters uncertainty are not related to observational errors (Buckland et al. 2007), thus is not related to the accuracy of the monitoring data which I concentrated on. However it was important to ensure that migration did not impact my closure assumption throughout the summer field season. This was supported by the 97.6% of VHF collared females, closely tracked (every second-third days) in summer of 1999 and 2000 (Hansen et al. 2009) staying within their respective study sites. In addition, Hansen et al. (2010b) supported that migration mainly occurred during winter.

The more information, the more precise the abundance estimate

My study is in line with Schaub and Kéry (2012) which encourages the combination of information in hierarchical models to improve inferences in population ecology. Despite collecting data with different sampling methods and having different uncertainties, when all of the my available data “shared strength” (Schaub and Kéry 2012) in a common model, the resulting estimates were more precise (Figure 4; Table 4) (see Gopaldaswamy et al., 2012, for another example of significantly improved tiger density estimates by combining two sampling methods in the same model).

Long time-series or repeated censuses increase the precision of estimates (Sæther et al. 2007, Dennis et al. 2010, Knape et al. 2013). Likewise, in Adventdalen, the increase in

precision resulting from repeated TC was minimal because single annual count brought enough information in the state-space model. Regardless of the length of the time-series, if a count was missing, the high annual fluctuation of the reindeer population led to low precision of abundance and growth rate estimates. Therefore, annual monitoring is crucial.

Total Counts accuracy

Total Counts accuracy can broadly vary depending on the studied species, type of landscape and observer effort. Loison et al. (2006) calculated an index based on TC repeats of chamois (*Rupicapra sp.*). In their study environment, the index was shown reliable and comparable to capture mark recapture if enough repeats were conducted. In my study system, during a monitoring census of August 2000, 100% (n=27) of adult female reindeer with VHF collar were sighted. These females were tracked before the census and known as present in Brøggerhalvøya and Sarsøyra. This demonstrated high detectability of at least adult females when using TC. However, some repeated TC had unexpected abundance differences e.g. on Sarsøyra in 2013 one repeat was outside the estimated CI (241 reindeer were counted while 223 [209:237] were estimated).

The main sources of errors to be accounted for were related to the observer, reindeer fur color, and weather variability. Indeed sighting effort and the observer experience could matter despite observers switching routes between repeats. Moreover, reindeer kept their white winter coats until mid-July, and were easier to detect than with the dark summer fur i.e. the count on Sarsøyra previously mentioned was the 1st TC conducted the 7th of July 2013. Animals were often scared off during windy days which facilitated detection but made it more difficult to keep track of animals position. Reindeer could be missed (false negative) but also double counted (false positive) by the same or another observer, or through animal movement when the site needed two days (Brøggerhavøya) or more (Adventdalen) to be covered. Systematic bias caused by false positive could only be quantified in summer 2000 where only

1.9% (n=53) of marked animals sighted during the census were counted twice. Nonetheless I expected this error to also be minor other years. In any case, I considered false positive and negative issues in our model by integrating TC in the state space model with a Poisson-Poisson sampling.

Ahrestani et al. (2013) analyzed process and observation error in 55 globally distributed populations of *Cervus* and *Rangifer* (27 and 28 respectively). They showed that “more-or-less” closed populations, that have been “carefully” monitored for decades, had low process observation error and great precision. Although process observation error cannot be quantified in the Poisson-Poisson state-space model, my study system followed these criteria and supports my judgment that TC estimates, especially when repeated TC were combined, were precise and could be assumed to have a low bias. I therefore could use TC as a reliable baseline for the comparison of DS estimates.

Distance Sampling sources of errors: detection function

Following DS model selection blindly would have led to biased estimates. According to the model selection, DS detection probability seemed to depend on the study site sampled (Table 3 and Figure 3. b and c). However, the similarity of landscape characteristics, methodological and analytical protocols in the two sites did not suggest such a difference. Availability for detection (i.e. the animal is in view) was expected to be similar inside the line transects covered area (Buckland et al. 2004) because of the wide plain with prostrated vegetation characteristics. Moreover, perceptibility (i.e. detection of the animal available for detection) was also expected similar. Indeed, the same single observer covered both sites and counts were stopped if weather prevented good visibility. In Kaffiøyra the last DS survey was conducted on the 25-26th of July 2013. At that time the reindeer had their darker summer fur, which was harder to spot in the landscape. Although this could explain why fewer animals were apparently detected from long distance on Kaffiøyra than Sarsøyra, it should not make a

difference in detection probability close to the line. The DS model did not account for cluster size influencing detection even though larger groups are expected to be detected at a longer distance (Buckland et al. 2004). This problem was reduced by data truncation so that the mean group size was low and did not differ between sites ($\bar{S} = 1.68$ group size in Sarsøyra and $\bar{S} = 1.58$ in Kaffiøyra with 5% truncation). Certainly, developing models and software that consider quantitative covariates at the observation level would improve DS method accuracy (see Amundson et al. in press, for an example regarding individual heterogeneity in detection).

However, data quantity could cause differences in the fit of detection curves. Ideally, a minimum of 60-80 observations are required to get adequate fit of the detection curve (Buckland et al. 2001), which was largely exceeded when both sites observations were pooled but not satisfied when Kaffiøyra was separately considered. Although both sites, combined or not, displayed uniform distribution of cluster with a low sample size variance (Appendix I), it is inherent that if few animal are observed, estimated density will be imprecise. Stochasticity of the animal position is more likely to modify the shape of the histogram when sample size is low (Figure 3). Additionally, Buckland et al., (2001) claims that the “shape criterion” is to some extent an assumption of distance sampling. This means detection function should have a “shoulder” shape close to the line, ensuring no movement of the animal toward or away from the observer and that detection remains certain over a small distance from the line. This assumption was fulfilled when data from both sites were pooled (Figure 3).

Royle et al. (2004) outlines that making “*a priori* judgment” about the most sensible way to partition variance (i.e. potential predictor covariates) could minimize the possibility that a covariate affects detection and abundance at the same time. Otherwise, the covariate effect would be sensitive to model structure. This scenario was similar to model Hn_21 where the study site was a covariate of both detection and density. Moreover, this model resulted in

a larger number of parameters than model Hn_8 (study site does not affect the detection) (Table 4). Accordingly, the $\Delta AICc$ showed a close to negligible difference between the two models.

These arguments justify why I considered estimates from model Hn_8 (pooled data from both regions to estimate the detection function) biologically reliable instead of Hn_21 (separate regions data set).

Distance Sampling source of error: habitat structure

Habitat structure could become an important source of bias if not accounted for (Pedersen et al. 2012, Sillett et al. 2012). DS results from Hn_8 gave higher abundance estimates than TC in both regions. The covered areas contained slightly more vegetated grounds than the total study area, with only 3.5 % difference both in Sarsøyra and Kaffiøyra. However, density of animals was so strongly linked to vegetation presence (Table 3) that this difference likely explained the small overestimation (Appendix V). If the difference in vegetated surface inside vs. outside the covered area was larger, the challenge to address both “spatial sampling and observation error” would not have been resolved (Yoccoz et al. 2001, Sillett et al. 2012). Anticipating such a scenario would avoid the possible need of adaptive distance sampling (Buckland et al. 2004).

Others argue that random placement of the line is reportedly inefficient if the zone of high density can be predicted (Buckland et al. 2004, Barabesi and Fattorini 2013). Barabesi and Fattorini, (2013) propose a stratified sampling method where random (for an example see Aars et al. 2009), or systematic lines (simpler to implement in the field) are placed inside congruent polygons that cover the study site. However, systematic design cannot have unbiased variance, yet, Fewster et al. (2009) has developed estimators of encounter rate variance that promote such design. Definition of stratum is difficult when vegetated and non vegetated surfaces occur along the same transect. A simple alternative would be to survey

additional transects until the vegetation proportion of the covered area is representative of the total study site.

It could be argued that heterogeneity in habitats introduce bias to the assumption of uniform distribution as well as uniform coverage probability (Buckland et al. 2004). However, modeling detection and density as a function of habitat covariates overcomes the need to separate density estimates into stratum that have low observations (such as non vegetated ground) (Buckland et al. 2004). In addition, contrary to Royle et al. (2004), vegetation coverage did not affect detectability in the model Hn_8 selected, and similar to their study, bootstrap goodness-of-fit did not show any significant lack of fit, concluding that no other heterogeneity should affect detection.

Future implications

The simplicity of the Svalbard tundra ecosystem should give similar count precision between both sampling methods. The sensitivity of the DS detection function to numbers of observations should serve as a warning to other monitoring programs using this sampling method, especially if additional assumptions are not met. I support choosing the upper limit outlined by Buckland et al. (2001) with a minimum number of 80 observations (for line transect). If enough transects are surveyed to represent the total vegetation coverage, distance sampling is a promising method to estimate reindeer density in other open tundra landscape. The DS method demonstrated in this study will be proposed to be used by the Governor of Svalbard, which manage Svalbard reindeer populations and conduct annual line transects. TC might not be possible across large study areas due to high demands for resources and logistics. Therefore reindeer abundance assessment across a wider spatial scale of the Svalbard archipelago could combine data from sites monitored by TC and others by DS (for an example see Aars et al. 2009). In such cases, TC should only be conducted in populations

assumed to be closed and with a high sampling effort to achieve the high precision as demonstrated in this study.

More accurate estimates led to easier detection of the effects of environmental drivers on population dynamics (Clark and Bjørnstad 2004, Knape et al. 2013), e.g. the effect of the temperature increase in the high Arctic (Constable et al. 2014). Investigating uncertainties and sources of error in wildlife monitoring with reliable statistical models (Buckland et al. 2007) strengthens inferences and, thus, permit to sustainably manage an ecosystem under increasing human pressure. The Bayesian state-space model illustrated in the present study and showed flexibility (Clark and Bjørnstad 2004, Kery and Schaub 2012) through its adaptation to the specificity of my study for estimating sampling methods uncertainties. Applying such analysis with the integration of biological parameters and age structure is promising for reindeer population dynamic studies under an increasing pressure of ROS events. Furthermore, it would improve ecosystem dynamics understanding, and improve our ability to fully explore the “early warning system” (Hansen et al., 2013), that is Svalbard in the light of a changing climate.

Conclusion

The present study assessed uncertainty in population counts of Svalbard reindeer, leading to useful population monitoring and management improvements. The open landscape and closed study locations (during a field season) resulted in fairly precise abundance estimates when monitored by TC. Nonetheless, large annual fluctuations in reindeer population size due to environmental stochasticity, density-dependence and migration require that censuses are conducted every year. Censuses were precise, yet quantification of counts' bias was not possible. However, bias was assumedly low once TC's were integrated into the state-space model and related to re-sightings of collared animals. Because of sample size issue, reindeer population size would have been wrongly estimated using the DS method alone if TC could not have been used as background information. Based on the results of this study, I strongly recommend that DS line transects conducted in this and other wildlife systems are based on a large number of observations ($n > 80$) in order to obtain robust detection functions. Further, sufficient transect lines should ensure that the habitat structure surveyed is representative of the total study site characteristics. This study has illustrated the flexibility of the Bayesian state-space modeling framework that maximizes the use of available data, even with wide CI, to increase the precision of population counts. Such simple models greatly improve population ecological inferences.

References

- Aanes, R., B.-E. Sæther, F. M. Smith, E. J. Cooper, P. A. Wookey, and N. A. Øritsland. 2002. The Arctic Oscillation predicts effects of climate change in two trophic levels in a high-arctic ecosystem. *Ecology Letters* 5:445–453.
- Aanes, R., B.-E. Sæther, E. J. Solberg, S. Aanes, O. Strand, and N. A. Øritsland. 2003. Synchrony in Svalbard reindeer population dynamics. *Canadian Journal of Zoology* 110:103–110.
- Aanes, R., B.-E. Sæther, and N. A. Øritsland. 2000. Fluctuations of an introduced population of Svalbard reindeer: the effects of density dependence and climatic variation. *Ecography* 23:437–443.
- Aars, J., T. A. Marques, S. T. Buckland, M. Andersen, S. Belikov, A. Boltunov, and Ø. Wiig. 2009. Estimating the Barents Sea polar bear subpopulation size. *Marine Mammal Science* 25:35–52.
- Abadi, F., O. Gimenez, R. Arlettaz, and M. Schaub. 2010. An assessment of integrated population models: bias, accuracy, and violation of the assumption of independence. *Ecological Society of America* 91:7–14.
- Ahrestani, F. S., M. Hebblewhite, and E. Post. 2013. The importance of observation versus process error in analyses of global ungulate populations. *Scientific reports* 3:3125.
- Amundson, C., J. A. Royle, and C. M. Handel. In press. A hierarchical model combining distance sampling and time removal to estimate detection probability during avian point counts. *The Auk*.
- Barabesi, L., and L. Fattorini. 2013. Random versus stratified location of transects or points in distance sampling: theoretical results and practical considerations. *Environmental and Ecological Statistics* 20:215–236.
- Brook, B. W., J. J. O’Grady, A. P. Chapman, M. A. Burgman, H. R. Resit Akcakaya, and R. Frankham. 2000. Predictive accuracy of population viability analysis in conservation biology. *Nature* 404:385–7.
- Brooks, S. P., E. A. Catchpole, and B. J. T. Morgan. 2000. Bayesian animal survival estimation. *Statistical Science* 15:357–376.
- Buckland, S. T., D. R. Anderson, K. P. Burnham, J. L. Laake, D. L. Borchers, and L. Thomas. 2001. *Introduction to distance sampling*. Oxford University press, Oxford, UK.
- Buckland, S. T., D. R. Anderson, K. P. Burnham, and L. Thomas. 2004. *Advanced Distance Sampling: Estimating Abundance of Biological Populations*. Oxford University Press, Oxford, UK.
- Buckland, S. T., K. B. Newman, C. Fernández, L. Thomas, and J. Harwood. 2007. Embedding Population Dynamics Models in Inference. *Statistical Science* 22:44–58.

- Burnham, K. P., and D. R. Anderson. 2002. *Model selection and inference: a practical information-theoretic approach*. Third edition. Springer, New York, USA.
- Claeskens, G., and N. L. Hjort. 2008. *Model selection and model averaging*. Cambridge Univ Press, Cambridge, UK.
- Clark, J. S., and O. N. Bjørnstad. 2004. Population time series: process variability, observation errors, missing values, lags, and hidden states. *Ecology* 85:3140–3150.
- Constable, A., A. Hollowed, N. Maynard, P. Prestrud, T. Prowse, and H. Stone. 2014. Polar regions. Chapter 28 *in* IPCC, 2014: *Climate Change 2014: Impacts, Adaptation, and Vulnerability*. Contribution of Working Group II to the Fifth Assessment Report of Intergovernmental Panel on Climate Change. Cambridge Univ Press, Cambridge, UK.
- Cressie, N., C. A. Calder, J. S. Clark, J. M. Ver Hoef, C. K. Wikle, E. Applications, S. Clark, M. Jay, and K. Wikle. 2009. Accounting for Uncertainty in Ecological Analysis: the Strengths and Limitations of Hierarchical Statistical Modeling. *Ecological applications* 19:553–570.
- Dennis, B., J. M. Ponciano, and M. L. Taper. 2010. Replicated sampling increases efficiency in monitoring biological populations. *Ecology* 91:610–20.
- Derocher, A. E., Ø. Wiig, and G. Bangjord. 2000. Predation of Svalbard reindeer by polar bears. *Polar Biology* 23:675–678.
- Elvebakk, A. 1997. Tundra diversity and ecological characteristics of Svalbard. Pages 347–359 *in* F. E. Wielgolaski, editor. *Ecosystems of the World*. Third edition. Elsevier, Amsterdam, NL.
- Fewster, R. M., S. T. Buckland, K. P. Burnham, D. L. Borchers, P. E. Jupp, J. L. Laake, and L. Thomas. 2009. Estimating the encounter rate variance in distance sampling. *Biometrics* 65:225–36.
- Fiske, I. J., and R. B. Chandler. 2011. unmarked: An R Package for Fitting Hierarchical Models of Wildlife Occurrence and Abundance. *Journal of statistical software* 43.
- Gaillard, J.-M., M. Festa-bianchet, and N. G. Yoccoz. 2001. Not All Sheep Are Equal. *Science* 292:1499–1500.
- Gopalaswamy, A. M., J. A. Royle, M. Delampady, J. D. Nichols, K. U. Karanth, and D. W. Macdonald. 2012. Density estimation in tiger populations: combining information for strong inference. *Ecology* 93:1741–51.
- Guillera-arroita, G., M. S. Ridout, B. J. T. Morgan, and M. Linkie. 2012. Models for species-detection data collected along transects in the presence of abundance-induced heterogeneity and clustering in the detection process. *Methods in Ecology and Evolution* 3:358–367.

- Hansen, B. B., R. Aanes, I. Herfindal, J. Kohler, and B.-E. Sæther. 2011. Climate, icing, and wild arctic reindeer: past relationships and future prospects. *Ecological Society of America* 92:1917–1923.
- Hansen, B. B., R. Aanes, I. Herfindal, B.-E. Sæther, and S. Henriksen. 2009a. Winter habitat–space use in a large arctic herbivore facing contrasting forage abundance. *Polar Biology* 32:971–984.
- Hansen, B. B., R. Aanes, and B.-E. Sæther. 2010a. Feeding-crater selection by high-arctic reindeer facing ice-blocked pastures. *Canadian Journal of Zoology* 88:170–177.
- Hansen, B. B., R. Aanes, and B.-E. Sæther. 2010b. Partial seasonal migration in high-arctic Svalbard reindeer (*Rangifer tarandus platyrhynchus*). *Canadian Journal of Zoology* 88:1202–1209.
- Hansen, B. B., V. Grøtan, R. Aanes, B.-E. Sæther, A. Stien, E. Fuglei, R. a Ims, N. G. Yoccoz, and A. Ø. Pedersen. 2013. Climate events synchronize the dynamics of a resident vertebrate community in the high Arctic. *Science* 339:313–315.
- Hansen, B. B., I. Herfindal, R. Aanes, B.-E. Saether, and S. Henriksen. 2009b. Functional response in habitat selection and the tradeoffs between foraging niche components in a large herbivore. *Oikos* 118:859–872.
- Johansen, B. E., S. R. Karlsen, and H. Tømmervik. 2012. Vegetation mapping of Svalbard utilising Landsat TM/ETM+ data. *Polar Record* 48:47–63.
- Kery, M., and M. Schaub. 2012. Bayesian population analysis using Winbugs: A Hierarchical Perspective. Academic Press, Waltham, MA.
- Knape, J., P. Besbeas, and P. De Valpine. 2013. Using uncertainty estimates in analyses of population time series. *Ecological Society of America* 94:2097–2107.
- Kohler, J., and R. Aanes. 2004. Effect of Winter Snow and Ground-Icing on a Svalbard Reindeer Population: Results of a Simple Snowpack Model. *Arctic, Antarctic, and Alpine Research* 36:333–341.
- Lebreton, J.-D., and O. Gimenez. 2012. Detecting and Estimating Density Dependence in Wildlife Populations. *Wildlife Management*.
- Lindén, A., and J. Knape. 2009. Estimating environmental effects on population dynamics: consequences of observation error. *Oikos* 118:675–680.
- Loison, A., J. Appolinaire, J. Jullien, and D. Dubray. 2006. How reliable are total counts to detect trends in population size of chamois *Rupicapra rupicapra* and *R. pyrenaica*? *Wildlife Biology* 12:77–88.
- Marques, F. F. C., and S. T. Buckland. 2003. Incorporating covariates into standard line transect analyses. *Biometrics* 59:924–35.

- Marques, T. A., S. T. Buckland, R. Bispo, and B. Howland. 2012. Accounting for animal density gradients using independent information in distance sampling surveys. *Statistical Methods & Applications* 22:67–80.
- Marshall, K. N., D. J. Cooper, and N. T. Hobbs. 2014. Interactions among herbivory, climate, topography and plant age shape riparian willow dynamics in northern Yellowstone National Park, USA. *Journal of Ecology* 102:667–677.
- Morellet, N., J.-M. Gaillard, A. J. M. Hewison, P. Ballon, Y. Boscardin, P. Duncan, F. Klein, and D. Maillard. 2007. Indicators of ecological change: new tools for managing populations of large herbivores. *Journal of Applied Ecology* 44:634–643.
- Morellet, N., F. Klein, E. Solberg, and R. Andersen. 2011. The census and management of populations of ungulates in Europe. Pages 106–143 *in* R. Putman, M. Apollonio, and R. Andersen, editors. *Ungulate management in Europe: problems and practices*. Cambridge Univ Press, Cambridge, UK.
- Muhlfeld, C. C., M. L. Taper, D. F. Staples, and B. B. Shepard. 2006. Observer Error Structure in Bull Trout Redd Counts in Montana Streams: Implications for Inference on True Redd Numbers. *Transactions of the American Fisheries Society* 135:643–654.
- Newman, K. B., S. T. Buckland, S. T. Lindley, L. Thomas, and C. Fernández. 2006. Hidden process models for animal population dynamics. *Ecological applications* 16:74–86.
- Pedersen, Å. Ø., B.-J. Bårdsen, N. G. Yoccoz, N. Lecomte, and E. Fuglei. 2012. Monitoring Svalbard rock ptarmigan: Distance sampling and occupancy modeling. *The Journal of Wildlife Management* 76:308–316.
- Poole, K. G., C. Cuyler, and J. Nymand. 2013. Evaluation of caribou *Rangifer tarandus* groenlandicus survey methodology in West Greenland. *Wildlife Biology* 19:225–239.
- Porteus, T., S. M. Richardson, and J. C. Reynolds. 2011. The importance of survey design in distance sampling: field evaluation using domestic sheep. *Wildlife research* 38:221–234.
- Reimers, E. 1983. Mortality in Svalbard reindeer. *Holarctic Ecology* 6:141–149.
- Rennert, K. J., G. Roe, J. Putkonen, and C. M. Bitz. 2009. Soil Thermal and Ecological Impacts of Rain on Snow Events in the Circumpolar Arctic. *Journal of Climate* 22:2302–2315.
- Royle, J. A., D. K. Dawson, and S. Bates. 2004. Modeling Abundance Effects in Distance Sampling. *Ecology* 85:1591–1597.
- Royle, J. A., and R. M. Dorazio. 2008. *Hierarchical modeling and inference in ecology*. Academic Press, San Diego, California, USA.
- Schaub, M., and M. Kéry. 2012. Combining information in hierarchical models improves inferences in population ecology and demographic population analyses. *Animal Conservation* 15:125–126.

- Seddon, P. J., K. Ismail, M. Shobrak, S. Ostrowski, and C. Magin. 2003. A comparison of derived population estimate, mark-resighting and distance sampling methods to determine the population size of a desert ungulate, the Arabian oryx. *Oryx* 37:286–294.
- Sillett, T. S., R. B. Chandler, J. A. Royle, M. Kery, and S. A. Morrison. 2012. Hierarchical distance-sampling models to estimate population size and habitat-specific abundance of an island endemic. *Ecological applications* 22:1997–2006.
- Singh, N. J., and E. J. Milner-Gulland. 2011. Monitoring ungulates in Central Asia: current constraints and future potential. *Oryx* 45:38–49.
- Solberg, E. J., P. Jordhøy, O. Strand, R. Aanes, A. Loison, B.-E. Sæther, and J. D. C. Linnell. 2001. Effects of density-dependence and climate on the dynamics of a Svalbard reindeer population. *Ecography* 24:441–451.
- Sutherland, W. J. 2006. *Ecological Census Techniques: A Handbook*. Second edition. Cambridge Univ Press, Cambridge.
- Sæther, B.-E., M. Lillegård, V. Grøtan, F. Filli, and S. Engen. 2007. Predicting fluctuations of reintroduced ibex populations: the importance of density dependence, environmental stochasticity and uncertain population estimates. *The Journal of animal ecology* 76:326–36.
- Tyler, N. J. C., M. C. Forchhammer, and N. A. Øritsland. 2008. Nonlinear effects of climate and density in the dynamics of a fluctuating population of reindeer. *Ecology* 89:1675–86.
- Van der Wal, R., and D. O. Hessen. 2009. Analogous aquatic and terrestrial food webs in the high Arctic: The structuring force of a harsh climate. *Perspectives in Plant Ecology, Evolution and Systematics* 11:231–240.
- Van der Wal, R., and A. Stien. In press. High arctic plants like it hot: a long-term investigation of between-year variability in plant biomass. *Ecology*.
- Williams, B. K., J. D. Nichols, and M. J. Conroy. 2002. *Analysis and management of animal populations*. Academic Press, San Diego, California, USA.
- Yoccoz, N. G., J. D. Nichols, and T. Boulinier. 2001. Monitoring of biological diversity in space and time. *Trends in Ecology & Evolution* 16:446–453.
- Zipkin, E. F., J. T. Thorson, K. See, H. J. Lynch, E. H. C. Grant, Y. Kanno, R. B. Chandler, B. H. Letcher, and J. A. Royle. 2014. Modeling structured population dynamics using data from unmarked individuals. *Ecology* 95:22–9.
- Øritsland, N. A. 1985. *Svalbardreinen og Dens Livsgrunnlag*. Norsk Polarinstitut, Tromsø.

Appendix I

Sample size variance

In respect to the Poisson distribution for which $\widehat{\text{var}}(\mathbf{n}) = E(n)$, possible clumping distribution of animals was assessed by calculating the sample size variance estimation $\frac{\widehat{\text{var}}(\mathbf{n})}{E(\mathbf{n})}$ that was expected close to 1 (Buckland et al., 2001; p109). This corresponded to the assumption that reindeers were randomly distributed along the different lines.

$$\widehat{\text{var}}(\mathbf{n}) = L \sum_{i=1}^k l_i \left(\frac{n_i}{l_i} - \frac{n}{L} \right) \times \left(\frac{1}{k-1} \right)$$

$$\widehat{se}(\mathbf{n}) = \sqrt{\widehat{\text{var}}(\mathbf{n})}$$

l_i represented the length of transect i , k the number of transects, n_i the number of observations per lines and n the sum of all n_i .

Table I. Sample size variance $\widehat{\text{var}}(\mathbf{n})$ and its standard deviation $\widehat{se}(\mathbf{n})$.

Area	$\widehat{\text{var}}(\mathbf{n})$	$\widehat{se}(\mathbf{n})$	$\frac{\widehat{\text{var}}(\mathbf{n})}{\mathbf{n}}$
Sarsøyra + Kaffiøyra	206.76	14.38	1.45
Sarsøyra	124.78	11.17	1.42
Kaffiøyra	83.96	9.16	1.53

Appendix II

Density estimation in Distance Sampling, theoretical explanations.

The detection probability required first that the cluster was available for detection and thus situated inside the covered area and then that it was detected by the observer (P_a). The covered area (a) in distance sampling corresponds to the area monitored from the lines. If a line was of length (L) and its width (ω) (including both sides of the line is of lengths 2ω), subsequently the covered area was of $2\omega L$ m² (meters is the measurement unit). The expected number of clusters λ_i was issued from random and independent observations. The density within the covered area of each partitioned line i corresponded to:

$$\widehat{D}_i = \frac{\lambda_i}{a_i \cdot Pa_i} = \frac{\lambda_i}{2L_i\omega \cdot Pa_i}$$

Buckland et al., (2001) introduced two related functions: the detection function $g(x_i)$ and the probability density function $f(x_i)$ of the perpendicular distance data x_i from the line i , related by the relation:

$$f(x_i) = \frac{g(x_i)}{\mu}$$

μ was the probability to detect an animal given that it was located in the ω width and corresponded to the area below the detection curve $g(x_i)$:

$$\mu = \omega \cdot Pa \quad \text{and} \quad \mu = \int_0^{\omega} g(x_i) dx$$

As all observation on the line were supposed to be detected: $g(0)=1$

$$\mu = \frac{g(x_i)}{f(x_i)} = \frac{1}{f(0)} \quad \text{and thus} \quad f(0) = \frac{1}{\int_0^{\omega} g(x_i) dx}$$

Finally (Marques and Buckland 2003),

$$\widehat{D}_i = \frac{\lambda_i}{2L_i\mu_i} = \frac{\lambda_i \cdot f(0)}{2L_i}$$

Appendix III

Model list

Table III. Model list names implemented with the **distsamp** function in Unmarked R package. Model respective detection key function (Hn= Half normal; Hz= Hazard rate, Unif= uniform) and covariates (α = detection covariates; λ = density covariates) are reported. Possible covariates were: the study site (site), the vegetation proportion (veg) inside the covered area, the logarithm of the veg (ln(veg)) and the quadratic polynomial of the logarithm value (ln(veg)²). Model list 1 corresponds to all 63 proposed models. Model list 2 correspond to a subset of 37 models from list 1 which did not have “site” as a possible detection covariate; models from model list 2 are highlighted in grey.

Name	Hn	Hz	α	λ	Name	Hn	Hz	α	λ
Hn	x	-	-	-					
Hz	-	-	-	-					
Unif	-	-	-	-					
Hn_1	x		site	-	Hz_31	x		site	-
Hn_2	x		Veg	-	Hz_32	x		veg	-
Hn_3	x		ln(veg)	-	Hz_33	x		ln(veg)	-
Hn_4	x		ln(veg) ²	-	Hz_34	x		ln(veg) ²	-
Hn_5	x		site + veg	-	Hz_35	x		site + veg	-
Hn_6	x		site * veg	-	Hz_36	x		site * veg	-
Hn_7	x		-	site	Hz_37	x		-	site
Hn_8	x		-	veg	Hz_38	x		-	veg
Hn_9	x		-	ln(veg)	Hz_39	x		-	ln(veg)
Hn_10	x		-	ln(veg) ²	Hz_40	x		-	ln(veg) ²
Hn_11	x		-	site + veg	Hz_41	x		-	site + veg
Hn_12	x		-	site + ln(veg)	Hz_42	x		-	site + ln(veg)
Hn_13	x		-	ln(veg) ²	Hz_43	x		-	ln(veg) ²
Hn_14	x		-	site * veg	Hz_44	x		-	site * veg
Hn_15	x		-	site * ln(veg)	Hz_45	x		-	site * ln(veg)
Hn_16	x		-	ln(veg) ²	Hz_46	x		-	ln(veg) ²
Hn_17	x		site	site	Hz_47	x		site	site
Hn_18	x		site	veg	Hz_48	x		site	veg
Hn_19	x		site	ln(veg)	Hz_49	x		site	ln(veg)
Hn_20	x		site	site * veg	Hz_50	x		site	site * veg
Hn_21	x		site	site + veg	Hz_51	x		site	site + veg
Hn_22	x		site + veg	veg	Hz_52	x		site + veg	veg
Hn_23	x		site + veg	site	Hz_53	x		site + veg	site
Hn_24	x		site * veg	veg	Hz_54	x		site * veg	veg
Hn_25	x		site + veg	site + veg	Hz_55	x		site + veg	site + veg
Hn_26	x		site * veg	site + veg	Hz_56	x		site * veg	site + veg
Hn_27	x		Veg	veg	Hz_57	x		veg	veg
Hn_28	x		Veg	site	Hz_58	x		veg	site
Hn_29	x		Veg	site + veg	Hz_59	x		veg	site + veg
Hn_30	x		veg	site * veg	Hz_60	x		veg	site * veg

Appendix IV

Table IV. Results from the Bayesian state-space model run in Winbugs for every state of the time-series of the four sub-populations. These models combined all TC available as well as DS estimates (see Table 1). At year t : \hat{N}_t = abundance; \hat{r}_t = growth rate. \bar{r} = average growth rate and σ_r^2 = process variance over the time-series. The mean posterior value is given with its standard deviation = sd, 95% credible interval [2.5%:97.5%] and coefficient of variation = CV. The chain convergence = Rhat.

Area	Parameter	t	mean	sd	2.5 %	97.5 %	Rhat	CV	
Brøgger	\hat{N}_t	1988	195.89	13.89	169.40	224.00	1.001	0.07	
	\hat{N}_t	1989	239.07	15.21	210.20	269.70	1.001	0.06	
	\hat{N}_t	1990	247.28	101.95	109.20	487.60	1.002	0.41	
	\hat{N}_t	1991	254.58	134.98	91.09	579.20	1.003	0.53	
	\hat{N}_t	1992	261.74	143.62	83.07	633.10	1.004	0.55	
	\hat{N}_t	1993	244.88	120.84	90.10	555.80	1.005	0.49	
	\hat{N}_t	1994	220.54	81.74	99.81	421.30	1.006	0.37	
	\hat{N}_t	1995	205.18	14.28	178.00	234.10	1.001	0.07	
	\hat{N}_t	1996	215.10	77.32	101.10	405.50	1.007	0.36	
	\hat{N}_t	1997	220.48	94.12	93.02	451.80	1.003	0.43	
	\hat{N}_t	1998	216.62	82.36	96.91	420.10	1.001	0.38	
	\hat{N}_t	1999	204.49	14.00	177.90	232.80	1.001	0.07	
	\hat{N}_t	2000	215.39	14.24	188.50	244.30	1.001	0.07	
	\hat{N}_t	2001	164.63	12.40	141.30	189.80	1.001	0.08	
	\hat{N}_t	2002	64.28	8.53	48.63	82.06	1.002	0.13	
	\hat{N}_t	2003	118.80	10.50	99.21	140.20	1.001	0.09	
	\hat{N}_t	2004	99.97	9.32	82.50	118.90	1.001	0.09	
	\hat{N}_t	2005	120.74	10.47	101.30	142.30	1.001	0.09	
	\hat{N}_t	2006	96.33	9.18	79.13	115.20	1.001	0.10	
	\hat{N}_t	2007	92.24	8.91	75.57	110.60	1.001	0.10	
	\hat{N}_t	2008	78.71	8.11	63.62	95.36	1.001	0.10	
	\hat{N}_t	2009	73.51	7.82	58.96	89.65	1.001	0.11	
	\hat{N}_t	2010	73.53	7.88	58.87	89.83	1.001	0.11	
	\hat{N}_t	2011	89.61	8.79	73.32	107.70	1.001	0.10	
	\hat{N}_t	2012	91.14	8.89	74.52	109.30	1.001	0.10	
	\hat{N}_t	2013	121.27	7.70	106.70	136.90	1.001	0.06	
		\hat{r}_t	1989	0.20	0.09	0.02	0.38	1.001	-
		\hat{r}_t	1990	-0.04	0.37	-0.78	0.71	1.002	-
		\hat{r}_t	1991	-0.01	0.36	-0.72	0.69	1.005	-
		\hat{r}_t	1992	0.01	0.38	-0.73	0.79	1.009	-
		\hat{r}_t	1993	-0.04	0.37	-0.83	0.68	1.002	-
		\hat{r}_t	1994	-0.06	0.37	-0.86	0.64	1.001	-
		\hat{r}_t	1995	-0.01	0.36	-0.71	0.71	1.006	-
	\hat{r}_t	1996	-0.01	0.34	-0.70	0.68	1.007	-	
	\hat{r}_t	1997	0.00	0.34	-0.69	0.69	1.003	-	
	\hat{r}_t	1998	0.00	0.35	-0.68	0.68	1.005	-	
	\hat{r}_t	1999	0.01	0.36	-0.71	0.74	1.001	-	
	\hat{r}_t	2000	0.05	0.09	-0.13	0.24	1.001	-	
	\hat{r}_t	2001	-0.27	0.10	-0.46	-0.08	1.001	-	
	\hat{r}_t	2002	-0.95	0.15	-1.26	-0.65	1.002	-	
	\hat{r}_t	2003	0.62	0.16	0.31	0.94	1.002	-	
	\hat{r}_t	2004	-0.17	0.13	-0.43	0.07	1.001	-	
	\hat{r}_t	2005	0.19	0.12	-0.05	0.44	1.001	-	
	\hat{r}_t	2006	-0.23	0.13	-0.47	0.02	1.001	-	
	\hat{r}_t	2007	-0.04	0.13	-0.30	0.21	1.001	-	
	\hat{r}_t	2008	-0.16	0.14	-0.43	0.11	1.001	-	
	\hat{r}_t	2009	-0.07	0.14	-0.35	0.21	1.001	-	
	\hat{r}_t	2010	0.00	0.14	-0.29	0.28	1.001	-	
	\hat{r}_t	2011	0.20	0.14	-0.08	0.48	1.001	-	
	\hat{r}_t	2012	0.02	0.13	-0.25	0.28	1.001	-	
	\hat{r}_t	2013	0.29	0.11	0.07	0.52	1.001	-	
	\bar{r}	-	-0.02	0.08	-0.18	0.14	1.001	-	
	σ_r^2	-	0.15	0.08	0.05	0.37	1.002	0.55	
	deviance	-	147.65	6.55	137.00	162.40	1.001	0.04	

Area	Parameter	t	mean	sd	2.5 %	97.5 %	Rhat	CV
Sarsøyra	\hat{N}_t	2000	154.25	11.98	132.00	178.50	1.001	0.078
	\hat{N}_t	2001	166.46	11.98	144.00	190.80	1.001	0.07
	\hat{N}_t	2002	117.30	10.67	97.45	139.10	1.002	0.09
	\hat{N}_t	2003	159.29	11.90	137.00	183.60	1.002	0.07
	\hat{N}_t	2004	152.67	11.46	130.60	175.70	1.001	0.08
	\hat{N}_t	2005	199.50	13.56	174.10	227.30	1.001	0.07
	\hat{N}_t	2006	162.20	11.61	140.00	185.70	1.001	0.07
	\hat{N}_t	2007	161.99	11.75	139.60	185.70	1.002	0.07
	\hat{N}_t	2008	169.48	12.02	146.90	194.00	1.001	0.07
	\hat{N}_t	2009	153.37	6.04	141.80	165.50	1.001	0.04
	\hat{N}_t	2010	127.33	10.56	107.10	148.60	1.002	0.08
	\hat{N}_t	2011	151.45	30.49	98.28	219.00	1.013	0.20
	\hat{N}_t	2012	175.46	12.41	151.90	200.50	1.001	0.07
	\hat{N}_t	2013	222.61	7.20	208.70	236.90	1.001	0.03
	\hat{r}_t	2001	0.08	0.10	-0.11	0.27	1.001	-
	\hat{r}_t	2002	-0.35	0.12	-0.58	-0.13	1.002	-
	\hat{r}_t	2003	0.31	0.12	0.09	0.54	1.003	-
	\hat{r}_t	2004	-0.04	0.10	-0.25	0.15	1.002	-
	\hat{r}_t	2005	0.27	0.10	0.08	0.47	1.002	-
	\hat{r}_t	2006	-0.21	0.10	-0.40	-0.02	1.001	-
	\hat{r}_t	2007	0.00	0.10	-0.19	0.20	1.001	-
	\hat{r}_t	2008	0.05	0.10	-0.14	0.24	1.002	-
	\hat{r}_t	2009	-0.10	0.08	-0.26	0.06	1.001	-
	\hat{r}_t	2010	-0.19	0.09	-0.37	-0.02	1.001	-
	\hat{r}_t	2011	0.16	0.20	-0.23	0.57	1.011	-
	\hat{r}_t	2012	0.16	0.20	-0.23	0.57	1.014	-
	\hat{r}_t	2013	0.24	0.08	0.09	0.39	1.001	-
\bar{r}	-	0.03	0.08	-0.13	0.18	1.001	2.71	
σ_r^2	-	0.08	0.05	0.02	0.21	1.001	0.69	
deviance	-	159.86	5.49	151.20	172.40	1.001	0.03	

Area	Parameter	t	mean	sd	2.5 %	97.5 %	Rhat	CV
Kaffiøyra	\hat{N}_t	2002	95.26	9.35	77.78	114.50	1.001	0.10
	\hat{N}_t	2003	124.29	9.97	105.6	144.70	1.001	0.08
	\hat{N}_t	2004	157.14	11.63	135.60	181.20	1.001	0.07
	\hat{N}_t	2005	159.90	11.98	137.70	184.60	1.001	0.07
	\hat{N}_t	2006	118.54	10.25	99.05	139.20	1.001	0.09
	\hat{N}_t	2007	124.77	10.17	105.40	145.20	1.001	0.08
	\hat{N}_t	2008	162.81	12.07	140.40	187.70	1.001	0.07
	\hat{N}_t	2009	155.28	8.50	139.10	172.50	1.001	0.05
	\hat{N}_t	2010	121.50	10.55	101.50	142.90	1.001	0.09
	\hat{N}_t	2011	133.52	33.29	77.47	209.80	1.003	0.25
	\hat{N}_t	2012	144.31	35.41	85.42	226.40	1.003	0.25
	\hat{N}_t	2013	152.35	10.45	132.40	173.30	1.001	0.07
	\hat{r}_t	2003	0.27	0.12	0.04	0.50	1.001	-
	\hat{r}_t	2004	0.24	0.10	0.04	0.44	1.002	-
	\hat{r}_t	2005	0.02	0.10	-0.17	0.21	1.001	-
	\hat{r}_t	2006	-0.30	0.11	-0.53	-0.08	1.001	-
	\hat{r}_t	2007	0.05	0.11	-0.16	0.27	1.001	-
	\hat{r}_t	2008	0.27	0.11	0.06	0.48	1.001	-
	\hat{r}_t	2009	-0.05	0.09	-0.22	0.13	1.001	-
	\hat{r}_t	2010	-0.25	0.10	-0.45	-0.05	1.001	-
	\hat{r}_t	2011	0.07	0.24	-0.42	0.56	1.004	-
	\hat{r}_t	2012	0.08	0.24	-0.39	0.55	1.003	-
	\hat{r}_t	2013	0.08	0.24	-0.39	0.57	1.003	-
\bar{r}	-	0.04	0.09	-0.14	0.23	1.001	-	
σ_r^2	-	0.09	0.07	0.02	0.28	1.001	0.84	
deviance	-	93.89	4.59	87.04	104.70	1.002	0.05	

Appendix V

Prediction of the density/abundance according to the proportion of vegetation present

Model Hn_8 issued from R package unmarked showed a strong correlation between density of reindeer and the proportion of vegetation present. Using the function *predict* (Fiske and Chandler 2011) it is possible to predict the density of reindeer with different magnitude of the covariate. Density was predicted for every decimal from 0 to 100% of vegetation cover in Figure V. In Table V, the same procedure was done to obtain density prediction for the total study area (0.66 and 0.50 vegetation proportion in Sarsøyra and Kaffiøyra respectively) and then was transformed to abundance of reindeer (see Methods). These estimates were very close to the one obtained by TC. It supported my hypothesis that the slight difference (3.5%) in vegetation proportion inside versus outside the covered area could explain the small overestimation of DS estimates found in my study (Table 3). Nonetheless, care should be taken when comparing these results because no bootstrap were conducted for the predictions of this appendix.

Table V: (1) DS abundance predicted according to the vegetation proportion of the total study area (not bootstrapped). (2) Results reported from Table 3; DS estimates where density was assumed constant inside and outside the covered area. (3) Results reported from TC estimates (four repeats for Sarsøyra) available in Table 4 and appendix IV.

Abundance	Sarsøyra	Kaffiøyra
(1) DS prediction	237 ± 26	150 ± 25
(2) DS extrapolation	256 ± 27	174 ± 19
(3) TC	221 ± 7	144 ± 13

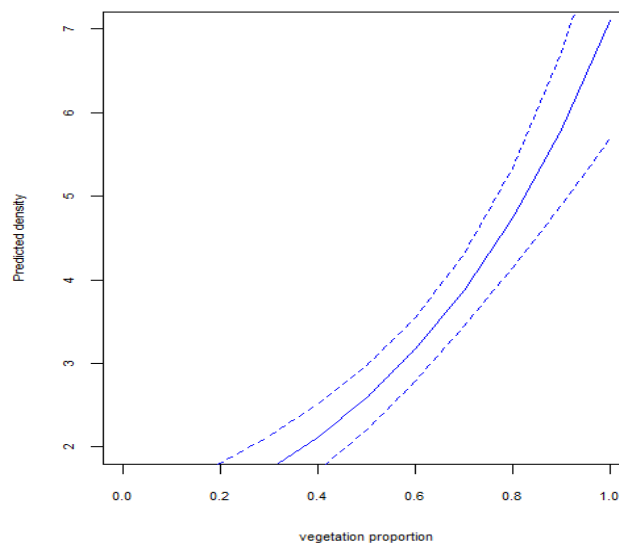


Figure V: Predicted density of reindeer as a function of vegetation proportion.

Supplements

R script available online for the following topics:

- 1) Distance sampling analysis in R package unmarked
- 2) Area calculation and extraction of vegetation covariate, spatial analysis
- 3) Winbugs script run from R, integration of TC time-series, repeated TC and DS. An example to measure Svalbard reindeer population size uncertainties on Sarsøyra.

Address:

<https://www.dropbox.com/sh/m62r702aikgn0kh/AAB5wovezNtWmNGaR4gO8ZOGa>

Articles referenced as “in press” can be requested at the following address:

mathilde@npolar.no